The Importance of Rheological Behavior in the Additive Manufacturing Technique Material Extrusion

Michael E. Mackay*
Department of Materials Science & Engineering
and
Department of Chemical & Biomolecular Engineering
University of Delaware
Newark, DE 19716, USA
(Dated: October 12, 2018)

Material Extrusion (ME), sometimes called Fused Deposition Modeling® (FDM) or Fused Filament Fabrication (FFF), is an additive manufacturing technique that places order 300 μm diameter molten polymer filaments sequentially onto a moving substrate to build an object. The feed material is a solid fiber that acts like a continuous piston in a heated barrel which plasticates itself to push molten material through a nozzle. The barrel pressure is substantial, of order 30 MPa ($\approx$4000 psi), and similar to that developed in contemporary polymer processing. The similarity does not end here with all the non-Newtonian and viscoelastic effects and heat transfer limitations that challenge extrusion operations coming to bear in ME. These will be discussed in this review with suggestions of areas of study.

I. INTRODUCTION

Over the millennia fabrication techniques were developed to manufacture objects through *Subtractive Manufacture* by taking raw material like; stone, wood or metal, and removing part of it to reveal the desired geometry. This could be the needed article or part of a larger collection that is assembled into the final product. A new manufacturing technology has been devised where instead of removing material it is added to an ever growing substrate and termed *Additive Manufacture* (AM).

The history of AM is brief and started in the 1980's with stereolithography [1] and then in 1991 *Fused Deposition Modeling*® (FDM®) was commercialized by Stratasys, this is the technology of concern here. FDM® is a trademarked phrase leading the RepRap community (RepRap is short for **Rep**licating **Rap**id-prototyper, meaning that 3D printers can replicate themselves) to invent the term *Fused Filament Fabrication* (FFF) that is not trademarked. However, the ISO and ASTM standard (ISO/ASTM 52900:2015) has used the term *Material Extrusion* (ME) to include FDM®/FFF technologies since ME is used whenever material is extruded through a nozzle. It is this terminology that is used here.

A summary of Additive Manufacturing technologies is given in Fig. 1. A solid, liquid or gaseous feedstock can be used to add material to the growing object using a variety of techniques with ME being that considered here. A fiber is the feedstock in ME that acts as a piston in a heated barrel that plasticizes itself to create the molten polymer. As the fiber is fed forward it generates pressure and the molten polymer is pushed into a nozzle and eventually outside to build the object. This technology is similar to the first injection molding machines invented by the Hyatt brothers over 100 years ago [2, 3]. Their invention consisted of a syringe-like pump that extruded plastic into a mold. ME does not have a mold and relies on surface tension and solidification to conserve the desired shape.

Noncrystalline polymers are almost exclusively used in ME, which includes slowly crystallizing polymers like poly(lactic acid) (PLA). The reason is simple, a fast crystallizing polymer, like polyethylene, will not allow the deposited polymer to weld with the substrate since the polymer chains will be tied to crystals. So, no mention of the melting enthalpy or the volume change on crystallization associated with semi-crystalline polymers is made in this review. Regarding the enthalpy, its inclusion would increase the energy required to melt the polymer although this energy is returned upon crystallization, both of which are simple to include in a nonisothermal analysis. The volume change upon crystallization is certainly a challenge since this could warp the object as the polymer crystallizes after deposition. This is one reason few semi-crystalline polymers are used in ME with another being that the viscosity can precipitously fall after melting to destabilize deposited filaments. With the exception of the later, these are not rheological effects, yet, none will be discussed below.

The extruder or *hot end* in ME is a remarkably simple device as shown in Fig. 2. The fiber is inserted into the fiber guide and pushed forward by a rotating gear or gears above the guide (not shown). Some ME instruments have the feed mechanism far from the hot end and not located on the printer saving weight to reduce print head inertia. In this case the fiber is inserted into a flexible sleeve to prevent buckling [5]. The fiber guide in Fig. 2 is surrounded by heat fins so the fiber does not melt at this point in the hot end.

Melting occurs in the threaded extension or *barrel* as it is surrounded by a heater block that is temperature controlled by the instrument. All melting occurs in the

* mem@udel.edu

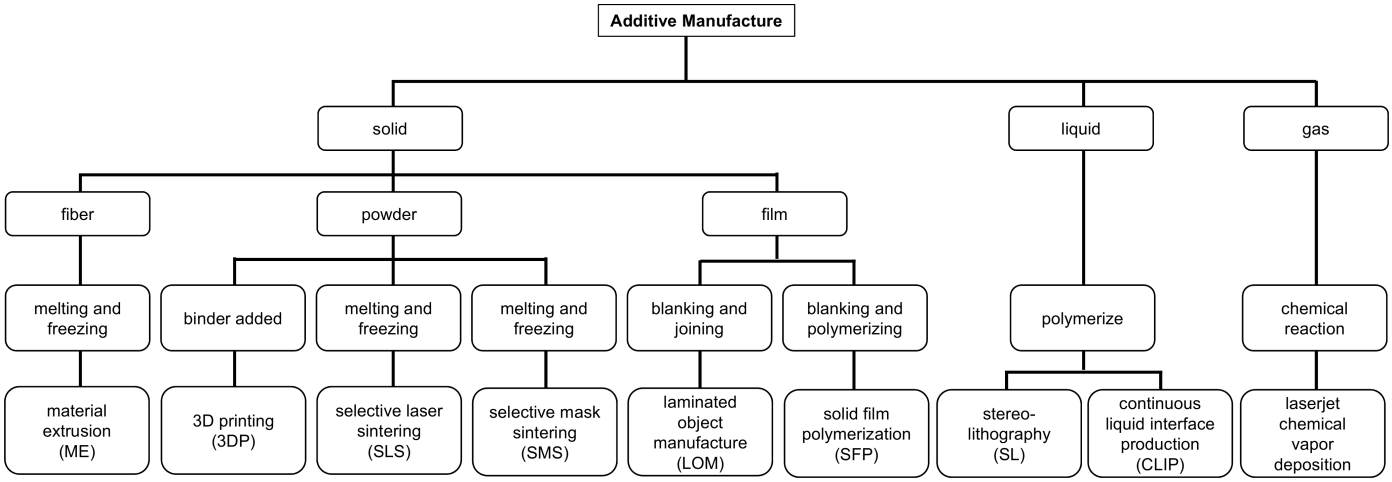

FIG. 1. Schematic showing the type of additive manufacturing technologies using a solid, liquid or gas feedstock. The solid feedstock can be in several forms with that for Extrusion Manufacture (EM), the technology of concern here, being a fiber that is melted, added to the object where it subsequently freezes. Adapted from Wendel *et al.* [4]

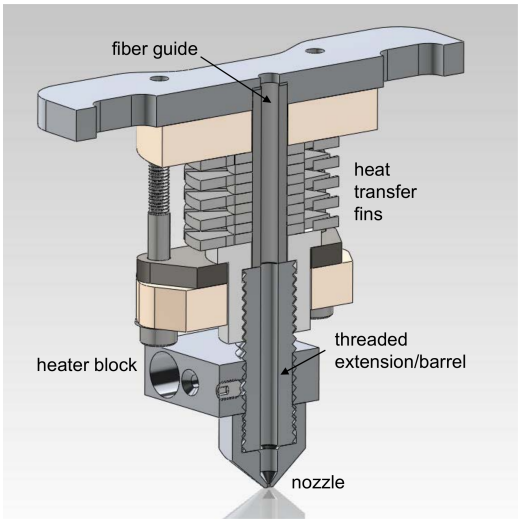

FIG. 2. The extruder or hot end used in a Taz 4. Image licensed CC BY-SA 4.0 International by Aleph Objects, Inc.

barrel over a length of order 30 mm. The molten polymer is then pushed into a conical nozzle where it exits through a small capillary with a diameter of approximately 0.5 mm.

Heat transfer is a limiting process in ME as discussed in detail by Go *et al.* [6] The challenge to increased heat transfer is partly due to the low thermal conductivity of polymers that is about 20 times smaller than water and 10,000 times lower than metals. However, it is the heat transfer coefficient for a non-Newtonian fluid that may be the limitation as discussed below in the next section entitled **Non-Newtonian fluid heat transfer**. Heat transfer from the barrel to the fiber is shown in Fig. 3 as an overview to the entire ME process.

The fiber diameter (D_f) is smaller than the barrel (D) and for one type of system the fiber is 2.85 mm in diameter while the inside barrel diameter is 3.175 mm (*i.e.* 1/8") leaving a gap of 0.16 mm which is small compared to the fiber diameter. Despite its small size there is certainly melt in the gap and the inset in Fig. 3 shows a likely shear flow pattern. Typical ME dimensions and process parameters are given in Table I.

The hot end or liquifier is an extruder and the shear flow pattern in the fiber - barrel gap is hypothesized to be reminiscent of that in a single screw extruder. In contemporary extruders, there is back mixing in the metering section and polymer is pushed forward by screw rotation and backwards by pressure along the helical flow path [7, 8]. Here the fiber is pushed forward to produce the drag flow while the pressure developed to extrude the polymer through the nozzle produces back flow. This affects the hot end performance and is discussed in more detail below in the section entitled **Extrusion**.

After the fiber is melted the polymer experiences shear and elongation upon entering the conical nozzle. This type of flow has a long history in the polymer processing industry mostly centered on polymer orientation and extrudate quality induced by the strong flow. At high enough flow rates the extrudate surface becomes rough and is called *sharkskin* while at even higher flow rates the melt becomes distorted as gross melt fracture occurs. The severity of this later distortion is affected by nozzle design and it is possible to extrude at higher rates if the design is changed [9]. Sharkskin is considered an exit instability, in other words it forms at the very exit of the nozzle, while gross melt fracture is affected by the entry flow conditions, both effects will be discussed in the section entitled **Flow in the nozzle**.

After the polymer exits the nozzle it is *released* from the confines of a flow geometry to have a free surface. When this occurs the diameter typically increases and is called die or extrudate swell. Even a Newtonian fluid

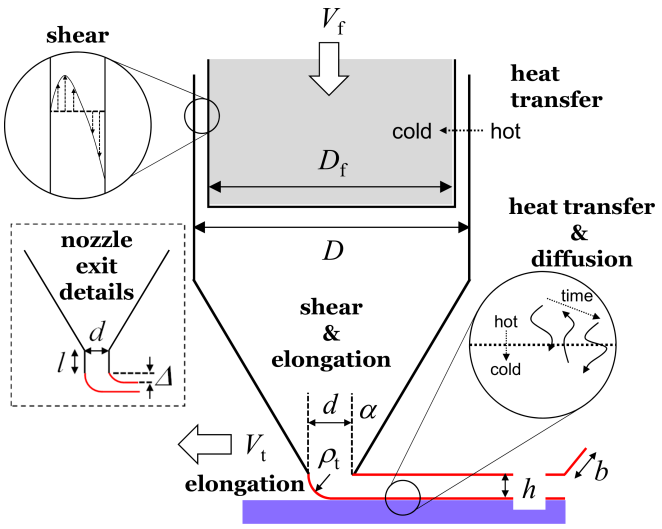

FIG. 3. The overall ME process. Heat transfer melts the fiber of diameter D_f fed at velocity V_f into a barrel with diameter D. Heat transfer occurs from the barrel to the fiber to melt the fiber. Pressure developed in the nozzle creates back flow between the fiber and barrel with a schematic of the shear flow shown. There is shear and elongation flow in the conical nozzle with half-angle α culminating with a capillary of diameter d (see the 'nozzle exit details' inset). Molten polymer is deposited onto the substrate by moving the nozzle/substrate at a velocity V_t to deposit a track of height h and width w. The melt makes a curved interface of curvature ρ_t that can create elongation. There is heat transfer and diffusion (reptation) as the molten track heats the substrate allowing diffusion to occur.

TABLE I. Typical parameter values in ME. The variables are shown in Fig. 3, the inset shows details about the nozzle exit and the associated parameters. The velocity V_d is the average velocity going out the nozzle through the capillary of diameter d. Many ME instruments have D_f equal to 1.75 mm.

Variable	Dimension with Units
D	3.175 mm
D_f	2.85 mm
d	0.3 - 0.5 mm
l	$\approx$ 0.5 mm
α	45°
Δ	$\approx$ 100 μm
h and b	$\approx$ 300 μm
V_f	0.625 mm/s
V_d	25 mm/s
V_t	40 mm/s

having no elasticity will swell at small Reynolds number, yet, elastic fluids like those used in ME will substantially swell. Even though this phenomenon has been studied for many decades the author believes a fresh look at die swell is in order particularly under conditions used in ME. A long capillary is not present in the 3D printer's nozzle to dampen entry effects and die swell will be influenced by upstream conditions that may induce a large increase in diameter. Since precise control of the deposited material is imperative die swell should be considered in the control software, or at least it should be accounted for when a material is developed for ME. The factors that influence the extrudate diameter are discussed in the section entitled **Die swell**.

After deposition the top track must heat the track below it above the glass transition temperature. The interface can then heal as polymer molecules diffuse across it to approach bulk behavior. An original manuscript by Wool and O'Conner [10] described the theory to relate the healing time to the reptation time which was later modified to the more relevant nonisothermal conditions encountered in ME by Yang and Pitchumani [11] and will be discussed in the section entitled **Healing**.

The final section, entitled **Other considerations**, will provide a discussion on a couple of topics considered for decades in the polymer processing industry that are relevant to ME. They include filament break-up, polymer molecule orientation and addition of reinforcement materials to the matrix, all of which are important and have not been considered in the ME literature. A matter of nomenclature is this; the term *fiber* is reserved for the feed material while *filament* represents the melt extruded from the nozzle. Filament break-up therefore means the scission of the extruded melt. Also, another nomenclature note is the deposited polymer is called a *track* while some authors call the deposited material a *road*.

II. NON-NEWTONIAN FLUID HEAT TRANSFER

Increasing the speed of ME additive manufacture is of prime importance. Go *et al.* [6] have considered factors which limit the speed and one of the most important is heat transfer. Reference to Fig. 3 shows where initial heat transfer occurs in ME, the solid fiber with diameter D_f is heated as it enters the the barrel to generate the melt that is subsequently forced through the nozzle.

Heat transfer seems a topic that is not influenced by rheological behavior, yet, this is untrue. Research by Schowalter and co-workers [12–14] centered on the use of hot-film anemometry to determine the presence of slip in polymer solutions and melts. The anemometer was used to find a Nusselt number (a measure of heat transfer) as a function of shear rate to reveal slip occurred when extrudate distortion was present (extrudate distortion is discussed in the **Flow in the nozzle** section). These studies show heat transfer in non-Newtonian fluids is a function of shear rate, as is the case for Newtonian fluids, and it can change when the flow behavior changes, which is not the case for Newtonian fluids.

Specific to ME, we hypothesize that as the polymer melts a thin, molten film of polymer will form between the moving fiber and heated barrel to produce a seal (this

is discussed in the **Extrusion** section below). The question is, How does this affect heat transfer? The rheological properties of the fluid within the film will affect its flow behavior that will certainly influence heat transfer. The heat transfer coefficient, the dimensional Nusselt number, is presented below and it does not follow theoretical expectations which could be due to this phenomenon although a different explanation is offered. Only by a thorough study of heat transfer and an understanding of the flow of non-Newtonian fluids within such a system can lead to an explanation.

The fiber has two functions, it acts as a piston to generate pressure and as it *melts* it supplies the feedstock. Thus, the fiber is a continuous piston. Many materials used in ME are glassy that do not have a melting transition, so, the term melt refers to producing a liquid at the required processing temperature. During this fiber melting and pressurization process the feed material is heated by thermal contact with the heated barrel wall. However, as will be shown below, the extrudate temperature is well below the wall temperature.

The first injection molding machines met a similar challenge where polymer pellets were melted and driven into a mold in short time. A hydraulic ram pushed pellets within a heated barrel to generate the melt that was forced into the mold. Heat transfer was a difficulty, so, a *torpedo* was placed annularly (concentrically) within the barrel. The torpedo was a solid cylinder with profiled ends that sat in the center of the barrel forcing all the pellets/melt to the heated wall while simultaneously generating heat through viscous dissipation within the annulus. This technology worked well for many years until it was replaced by an extruder-like ram which could simultaneously turn like a plasticating extruder screw to generate a melt pool at its tip that was then pushed forward to fill the mold.

The design of future ME instruments may include a torpedo to promote a better temperature profile. This is a simple engineering solution that has a rich history in the polymer processing industry and should provide an improved material for 3D printing. If a torpedo is included in the instrument design then it could induce polymer orientation and have a positive effect on other aspects of ME considered below. This could be a fruitful area of research on how rheology and heat transfer can be improved to 3D print a superior object. On another tack, recently, Go and Hart [15] overcame the heat transfer limitation by using a near infrared diode laser to preheat the fiber before it entered the heated barrel to produce a printer that operated approximately 10 times faster. Since no such commercial instrument exists with either of these technologies, heat transfer of a material simply convected in a cylinder is considered here.

We have found the outlet temperature is much less than the barrel/threaded extension wall temperature even at small flow rates, sometimes of order 50°C lower [16]. The reason for this is best explained by determining the heat transfer coefficient. Equating the rate of heat flow using the first law of thermodynamics ($wC_p[T_{\rm out} - T_{\rm in}]$, w is the mass flow rate, C_p, the specific heat capacity, $T_{\rm in}$, the inlet (fiber) temperature and $T_{\rm out}$, the outlet temperature) to Newton's law of heat transfer ($h_a \pi DH \Delta T_a$, h_a is the average heat transfer coefficient determined using a given average temperature driving force ΔT_a, D, the barrel inside diameter and H, the barrel length). Assuming $\Delta T_a = \{[T_{\rm wall} - T_{\rm in}] + [T_{\rm wall} - T_{\rm out}]\}/2$ ($T_{\rm wall}$ is the barrel wall temperature) one finds

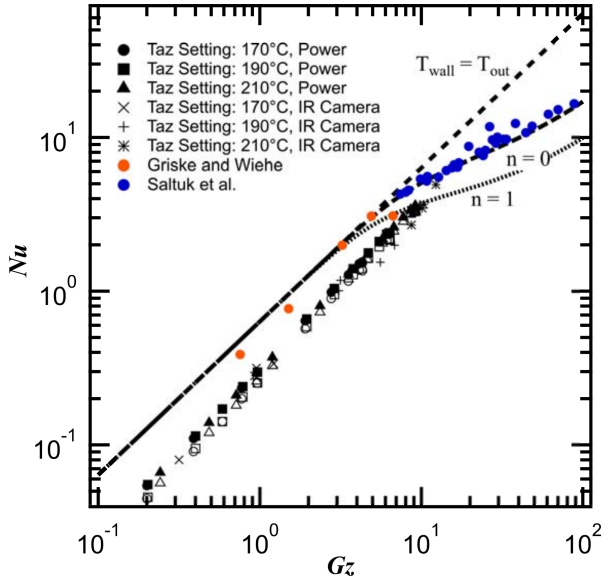

FIG. 4. Nusselt number – Graetz number graph showing the theoretical relations determined by Graetz for a power law index of zero or one (see McAdams [17], page 230) compared to the results of Griskey and co-workers [18, 19] and Phan *et al.* [16] who used different set point temperatures and methods to determine the outlet temperature.

$$Nu = \frac{2}{\pi} Gz \frac{\Theta}{2 - \Theta} \tag{1}$$

where Nu is the Nusselt number ($Nu \equiv h_a D/k$, k is the material's thermal conductivity), Gz, the Graetz number ($Gz \equiv wC_p/Hk$) and Θ, a dimensionless temperature ($\Theta \equiv [T_{\rm out} - T_{\rm in}]/[T_{\rm wall} - T_{\rm in}]$). Note Gz is equal to the Reynolds number Re multiplied by the Prandtl number Pr times H/D with $Re \times Pr$ being used in many heat transfer correlations. In an experiment one would know all the variables in the above equation except $T_{\rm out}$ which would be measured to determine Nu as a function of Gz. The derivation of Eq 1 is given in great detail by Phan *et al.* [16]

Equation (1) can be used to show what outlet temperature is possible and represents the maximum possible temperature that can be achieved. The predicted Nu as a function of Gz is given in Fig. 4 (see the Supporting Information and [17, 20] who discuss Graetz' prediction of Θ as a function of Gz.) and up to $Gz \approx 5$ the outlet tem-

perature is predicted to be equal to the wall temperature. This is represented by the equation $Nu = 2/\pi \times Gz$. However, at higher Gz the outlet temperature is predicted to be less than the wall temperature.

Validation of the model can be seen when the results of Griskey and co-workers [18, 19] for a viscoelastic polyethylene melt are compared to the model as shown in the figure. The polymer melt was supplied by a single screw extruder that fed a specially designed, heated die allowing the temperature profile to be measured. One can discern the model and data agree well, albeit the model with $n = 0$ compares better to the data. This could be due to the die being heated above the inlet temperature in the experiments. Under this condition, the fluid next to the wall would have a lower viscosity than towards the centerline promoting a velocity profile similar to plug-like (*i.e.* $n = 0$).

The data of Phan *et al.* gathered using a Taz 4 printer with PLA are also given in the figure and they do not agree with the model nor Griskey *et al.'s* data. They concluded fouling contributed to a reduction in the heat transfer coefficient. A typical 3D printer has different polymers forced through it and is a challenge to clean the heated barrel. It was observed there was degraded polymer in the barrel and this together with extrusion of different polymers contributed to inefficient heat transfer from the metal wall.

Fouling is a consideration that must be considered and protocols should be developed to reduce its effect. This is intimately linked with generating increased throughput since heat transfer is a limiting step in ME. Indeed the state-of-the-art for non-Newtonian fluid heat transfer was summarized by Metzner *et al.* [21] approximately 60 years ago! With new tools, like molecular dynamics, [22] and other theoretical considerations of polymers undergoing shear near wetting and non-wetting substrates [23] could provide rich results that when combined with experimental studies will modernize the heat transfer literature while centered on non-Newtonian flow in ME.

III. EXTRUSION

As discussed above, the fiber acts as a ram to push *itself*, as it melts, though the nozzle and eventually onto the substrate. There is a slight difference in the barrel and fiber diameters to have a gap B of approximately 200 μm between them, see Table I ($B \equiv [D - D_f]/2$), so, it is hypothesized polymer melt acts as a seal to generate large pressures that push the melt through the nozzle and out the very small diameter capillary.

Contemporary polymer extruders have a screw rotating in a cylindrical barrel with the helical motion of the screw exerting a *drag* flow forward toward the die. The solid polymer pellets are gradually melted as they are convected forward until eventually only a melt exists. This flow admits a positive pressure gain that opposes the drag flow allowing a counter pressure driven flow to develop along the helical axis. At equilibrium the drag flow is greater since mass is ultimately expelled from the die.

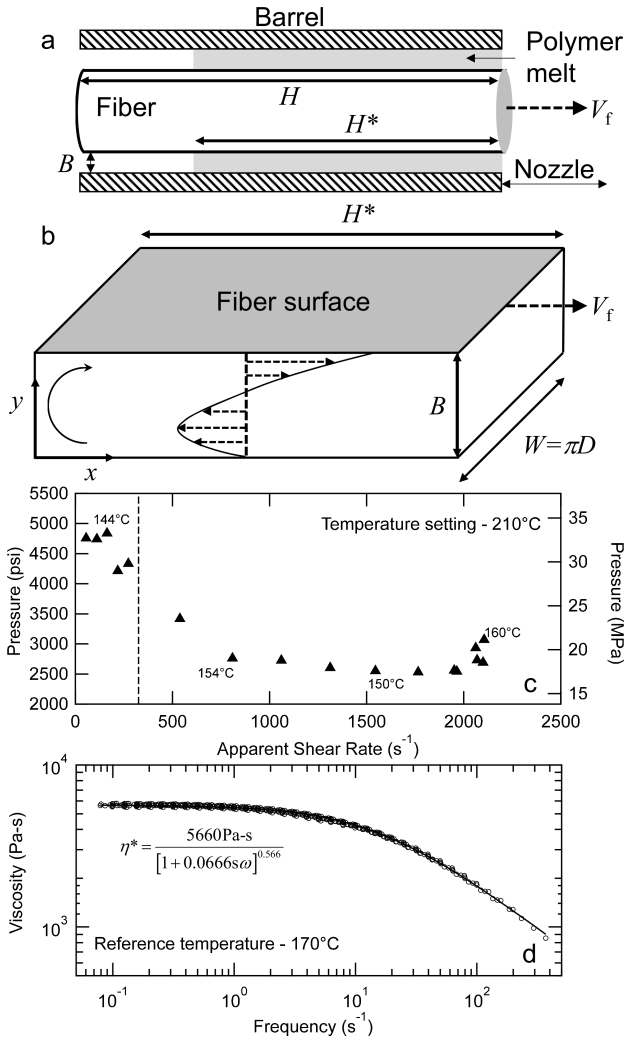

FIG. 5. (a) Drawing of the fiber feedstock entering the heated barrel (threaded extension) with an equilibrium height H^* of polymer melt hypothesized to make a pressure seal between the unmelted fiber and the barrel. (b) Schematic showing the hypothesized recirculating flow that develops between the barrel and fiber together with geometric and processing variables. (c) Pressure developed in the nozzle that forces the PLA melt through a 0.5 mm diameter nozzle with a temperature setting of 210°C on the Taz 4 printer. The vertical dotted line represents the shear (flow) rate used when making an object. The apparent shear rate is equal to $32Q/\pi d^3$ where Q is the volumetric flow rate and d is the nozzle's capillary diameter. Data from Phan *et al.* [16] (d) Complex viscosity as a function of frequency for PLA at a reference temperature of 170°C. The solid line through the data represents the equation in the graph, $\eta*$ is the complex viscosity and ω is the frequency. Data courtesy of D.D. Phan.

For the case at hand, the drag and pressure flows are equal to generate the seal between the fiber and barrel that rises to an equilibrium height H^* as shown in Fig. 5.

The height H^* must be smaller than the heated barrel (threaded extension) length H to be an effective seal. If $H^* > H$ then melt would extend into the unheated reagion above the barrel jamming the feeding mechanism. Also shown in the figure is the pressure developed in the nozzle that is approximately 4000 psi or 28 MPa which is substantial and the effective gap between the unmelted fiber and barrel must be small, and sealed.

The pressure shown in the graph was determined by monitoring the power to drive the counter-rotating gears that grip the fiber and force it into the nozzle [16], since power is pressure drop multiplied by volumetric flow rate (while accounting for efficiency) one can easily determine the pressure during ME operation. The curious shape of the graph is due to heat transfer summarized in Fig. 4; the rate of heat transfer (Nu) increases as the shear (flow) rate (Gz) increases causing the temperature to rise and the viscosity to fall. This leads to a lower pressure. The numbers next to some data points represent the extrudate temperature determined with an infrared camera demonstrating the temperature increase at greater rates. See Phan *et al.* for discussion of the accuracy of these temperature measurements.

Now that the pressure is known one can predict how high the melt progresses up the gap by realizing the drag and pressure flow act independent of each other. [24] Since the gap is small, curvature effects can be neglected and the drag flow velocity profile is written

$$v_\mathrm{d} = \frac{y}{B}\, V_\mathrm{f}$$

where the variables are shown in Fig. 5 and v_d is the velocity due to drag flow. The volumetric flow rate due to drag flow Q_d is easily found to be

$$\frac{Q_\mathrm{d}}{W} = \int_0^B v_\mathrm{d}\, dy = \frac{1}{2} B V_\mathrm{f} \tag{2}$$

The pressure driven velocity profile for a generalized Newtonian fluid (GNF) is

$$v_\mathrm{p} = \frac{nB}{2[1+n]} \left[\frac{B\,\Delta P}{2KH^*}\right]^{1/n} \left[1 - \left|\frac{2y*}{B}\right|^{1+1/n}\right]$$

where v_p is the velocity due to pressure flow, ΔP is the pressure drop along H^*, $y*$ is equal to $y - B/2$ and K and n are the GNF consistency index and power law. The volumetric flow rate due to the pressure drop Q_p is found by also integrating over the flow area

$$\frac{Q_\mathrm{p}}{W} = \frac{B^2}{2\,[2+1/n]} \left[\frac{B\,\Delta P}{2KH^*}\right]^{1/n} \tag{3}$$

At steady state the drag and pressure induced flow rates are equal, so, setting Eqs. (2) and (3) equal one finds the equilibrium height

$$H^* = \frac{B\,\Delta P}{2K} \left[[2+1/n]\,\frac{V_\mathrm{f}}{B}\right]^{-n} = \underbrace{\frac{B^2 \Delta P}{6\eta V_\mathrm{f}}}_{\mathrm{n=1}} \tag{4}$$

where η is the Newtonian viscosity (*i.e.* $n = 1$). The above equation can be used for either a GNF or a Newtonian fluid depending on the shear rate in the gap. The shear rate for drag flow is $\dot\gamma_\mathrm{d} = V_\mathrm{f}/B$ while the nominal shear rate for pressure flow is $\dot\gamma_\mathrm{p} = 3\dot\gamma_\mathrm{d}$. Using values in Table I one finds the shear rates are approximately 5 – 10 s^{-1} which is barely into the shear thinning regime for PLA shown in Fig. 5. The viscosity data are for a reference temperature of 170°C while the typical barrel temperature is 210° for PLA and taking the temperature in the gap close to the wall temperature makes the terminal viscosity equal to 560 Pa-s (the shift factor for PLA is given by $a_T = 6.98 \times 10^{-13}\, \exp(12,400/T(\mathrm{K}))$ where T is temperature).

Using either 170°C or 210°C finds h is approximately 35 mm or 350 mm, respectively, where both are larger than the barrel length of 28 mm. Clearly, this is a simple model and the predictions are suspect. It does highlight how little is known about this flow considering the 'piston' will gradually disappear as it is forced towards the exit suggesting B must change (increase) as the nozzle is approached.

Gilmer *et al.* [25] demonstrated this type of flow behavior (*i.e.* pressure and drag flow in the gap) was a challenge and determined that back flow in the extrusion region of the ME hot end or liquifier was indeed a limitation for these type of printers. They proposed a Flow Identification Number or FIN to determine when back flow was so large that the polymer would flow out of the heated region

$$\mathrm{FIN} = \frac{\Delta P/L}{\eta\, V_\mathrm{f}} \left[D^2 - D_\mathrm{f}^2\right] \neq \underbrace{\frac{\Delta P/H}{\eta\, V_\mathrm{f}} \left[D - D_\mathrm{f}\right]^2}_{\mathrm{eqn(4)}} \tag{5}$$

where L is a length given by Gilmer *et al.* that was not defined. The far right equation, after the not equal to sign, is Eq. (4) rearranged for a Newtonian fluid. They state if FIN is greater than approximately 200 the pressure flow would be greater than the drag and melt would be forced out of the heated region to stop extrusion. Using Eq. (4), as shown in Eq. (5), our definition of FIN simply shows if it is greater than one pressure flow is too great and melt would be forced out of the heated region.

Clearly, experimental and theoretical studies are needed to study this type of extrusion mechanism since it is unique and has not been considered before. It could have implications on material properties required for advanced operation and how the heat transfer is optimized to increase throughput. Since the 'piston' disappears during operation this could lead to some fascinating flow

patterns especially since the entire process is nonisothermal. For example, the fiber could have a conical shaped end during the melting process that will induce both shear and elongational rheological properties to promote an effective seal with a viscoelastic fluid. Finally, it is expected the cool fiber entering the barrel will play a role in the seal produced. In other words, the fiber will cool the melt promoting a higher viscosity and the ability to seal the device, this was not considered in the above analysis albeit taking a higher overall viscosity than suggested by the barrel wall temperature will have a similar effect.

Finally, there are many similaries between ME and contemporary extrusion, as mentioned above, allowing one to use older analyses and experience to rapidly advance ME. However, the highest shear rate in the ME barrel, which occurs between the unmelted fiber and the barrel, is much lower than that experienced in the metering section of a contemporary extruder. These are equivalent in that they provide the seal allowing pressurization of the melt downstream. The metering section shear rate is given approximately as $\pi D_{\text{ext}} N / B_{\text{ext}}$, where D_{ext} is the extruder barrel inside diameter (of order 150 mm for a production model extruder), B_{ext}, the gap between the root of the screw and the inside of the barrel (of order 6 mm and equivalent to B in Fig. 5), and N, the screw rotation rate (of order 1.7 rev/s). This leads to a shear rate of about 130 s^{-1} which is much lower than the 5 – 10 s^{-1} given above for the shear rate between the moving fiber and barrel. This could have implications for material selection in ME since the rheological properties should be tailored to create the best seal at this much lower shear rate compared to contemporary extrusion. So, any changes in rheological properties could affect the ME process in a way that is not apparent based on contemporary heuristics.

IV. FLOW IN THE NOZZLE

Flow of a polymer melt into a conical nozzle has been studied for decades and it is generally accepted that elongational flow properties are important in dictating the pressure drop [26, 27] and flow instabilities that may develop [28]. Nason reported [29] that after a certain pressure '... the extruded material becomes rough and wavy, and the effect increases as pressure is increased.' While this is certainly a challenge to all extrusion operations it is the appearance of sharkskin (see Fig. 6), or surface roughness, on the surface of the extrudate at lower pressures [30] that limits many manufacturing operations [9]. Whether sharkskin influences ME is open to debate, however, it is expected that this type of surface roughness will limit the adhesive strength of deposited filaments.

First, consider flow in a conical die as shown in Fig. 3 where the geometric variables are defined. Phan *et al.*, [16] following Cogswell's analysis, [26] determined the pressure drop in the die to be

$$P_\alpha = L \frac{2^{1-m} \tan(\alpha)^m}{3m} \dot{\gamma}_a^m + K \frac{2}{3n \tan(\alpha)} \left[\frac{1+3n}{4n} \right]^n \dot{\gamma}_a^n$$

where α is the die half-angle, L and m are the consistency index and power law for the elongational viscosity and $\dot{\gamma}_a$ is the apparent shear rate in the capillary at the cone exit ($\dot{\gamma}_a \equiv 32Q/\pi d^3$). The assumption of a GNF is made in deriving this pressure drop, yet, m does not have to equal n as required by this fluid model. Cogswell assumed $m = 1$ and L is merely the elongational viscosity assumed constant during flow in the cone for a given $\dot{\gamma}_a$.

The pressure drop due to reorganization of the melt from the converging region into the capillary can be estimated from the relation provided by Boles *et al.* [31] and Kwon *et al.* [32]

$$P_o = K \left[\frac{1+3n}{4n} \frac{32Q}{\pi d^3} \right]^n \frac{1.18}{n^{0.7}}$$

Finally, the pressure drop for flow through the short capillary is

$$P_c = K \left[\frac{1+3n}{4n} \frac{32Q}{\pi d^3} \right]^n \frac{4l}{d}$$

leading to the total pressure (P_{tot}) predicted by this model

$$P_{\text{tot}} = P_\alpha + P_o + P_c$$

Phan *et al.* successfully modeled pressure drop data for flow of PLA in an ME die using the above equation, however, it was not perfect. In fact, it was a challenge to shift the data at different temperatures in a nozzle having a short capillary (0.5 mm long by 0.5 mm diameter) at its exit (this was a die that mimicked the nozzle in a Taz 4 ME instrument and was mounted onto the end of an extruder so the polymer melt was under an isothermal condition). This must be due to the short capillary at the exit where the flow is not viscometric.

It will be a challenge to model flow in an ME instrument since the exit capillary will by definition be short and suggests new research endeavors in understanding such a flow. For example, the mindset must be centered on nonequilibrium, viscoelastic flow which will also bring challenges for material formulators. Furthermore, the above equations are found to all significantly contribute to the total pressure drop necessitating careful consideration of each component. How long or short should the exit capillary be? Does there need to be a capillary at all? (Pragmatically a capillary may have to be present since a sharp exit will be damaged when the nozzle hits the bed.) How much orientation induced by flow in the conical nozzle is present? Can this orientation be retained

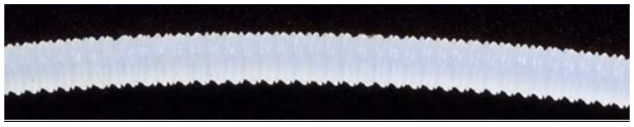

FIG. 6. Picture of sharkskin developed on a polyethylene fiber after extrusion through a capillary die attached to a single screw extruder.

in the printed object to increase strength? These are simple questions that require thought especially within the context of the already expansive polymer processing literature.

This leads to the formation of sharkskin that is suspected to influence ME operation and extruded object ultimate strength. Agassant *et al.* [9] give a good review of melt fracture and sharkskin instabilities and suggest some exit geometry changes and the use of additives to reduce sharkskin. A picture of sharkskin is shown in Fig. 6 for a polyethylene that developed when the shear stress in the capillary was approximately 0.1 MPa, this is a typical order of magnitude for the critical stress where sharkskin develops. Generally, a critical shear stress exists and not a critical shear rate so the processing rate can be enhanced by using a higher temperature. Eventually though the surface will become rough and this is undesirable for any extrudate, how this influences the adhesive strength of the 3D printed object is an open subject. Will it heal before solidifying? Should rheological properties be tailored to promote healing after the appearance of sharkskin?

The use of additives like fluoropolymers and other materials, even barium titanate particles, have been shown to reduce or even eliminate sharkskin. This leads to another avenue of investigation, will additives affect the object strength? As discussed in the section **Healing** below, the deposited strand must melt the object where it is placed then the macromolecules must diffuse and eliminate the interface. Will additives influence this process? Thus, one may be able to reduce sharkskin, yet, the ultimate part strength could be reduced if the molecular knitting process is affected. If it is found additives impart negative consequences then die design must be considered, however, the capillary will be extremely short. Thus, will sharkskin be influenced by upstream stresses? Finally, if sharkskin is eliminated will gross melt fracture limit the process? All these questions are worthy of study with a new emphasis on ME.

V. DIE SWELL

Precise placement of well defined tracks sequentially onto an ever growing substrate is critical to creating a part with high fidelity. The fiber is fed into the heated barrel *via* accurate stepper motors and spatially deposited to perhaps an accuracy of 50 – 100 μm. However, the extrudate diameter is not equal to the nozzle's diameter due to die or extrudate swell that can certainly influence object quality.

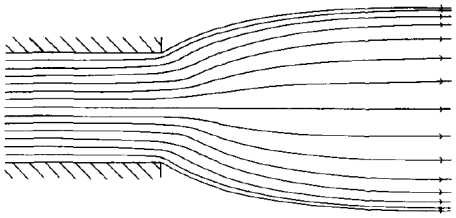

FIG. 7. Figure by Richardson (his Fig. 8) showing the likely streamline re-arrangement of a fluid after exiting a capillary [40]. Used with permission of Springer Nature.

Middleman and Gavis [33] showed the extrudate diameter relative to the nozzle χ for a Newtonian fluid can be represented as

$$\chi = 0.25 \times \exp\left(-\left[\frac{Re}{20}\right]^{1.39}\right) + 0.87$$

where Re is the Reynolds number (this is a numerical representation by the present author of graphically presented data). A Newtonian fluid shows a 12% diameter increase at low Re, due to streamline rearrangement after exiting the die, and a reduction at high Re. The high Re limit is simple to calculate using a momentum balance [24] while the other limit is slightly more involved. In addition, χ is affected by tube length for a given diameter and is suspected to be due to incomplete velocity profile development among other viscous effects [34].

Viscoelastic fluids, like those used in ME, have other factors that affect its final size. [35] Barus [36] found extrudate swelling in *marine glue* when extruded from a capillary[1] and concluded '... residual viscosity resembles a slowly reacting elasticity' while Merrington [37] stated '... elastic recovery commences at the actual capillary end' and contributed to swelling. See comments by Metzner on the accuracy of the above [38].

These statements led later researchers to consider how elasticity affected die swell using a couple of theoretical approaches culminating in Tanner's relation [39]

$$\chi = \left\{1 + \frac{1}{2}\left[\frac{N_1}{2\sigma}\right]^2\right\}^{1/6} + 0.13 \qquad (6)$$

where 0.13 was added onto the expression to agree with data in the terminal region (it is unclear if the value is 0.12 or 0.13 for a Newtonian fluid). The ratio of the first

[1] Marine glue is an organic solution of shellac and india-rubber or asphaltum.

normal stress difference N_1 to twice the shear stress 2σ is denoted as recoverable shear strain in accord with Barus' and Merrington's suppositions.

Tanner's expression has been tested and changed, however, ultimately, other expressions are similar [41]. The ideas of Richardson, [40] who published his work around the same time as Tanner originally did, are thought provoking and challenge the accepted die swell models. He shows in Fig. 7 that streamlines near the capillary walls must narrow after exiting the capillary. Since the fluid travels slowest while near the wall in the capillary upon exiting they must move closer together allowing the fluid to accelerate and obtain the extrudate average velocity. On the other hand, streamlines in the middle must move further apart since the fluid will slow after exiting. Thus, at least for a Newtonian fluid, the extrudate will swell from the 'inside out.'

Contemporary research should consider this observation. With the proliferation of accurate rheological characterization, advanced instrumentation for experimental studies, new rheological models and exacting numerical simulation a thorough study could reveal the fundamentals of swelling, even for a Newtonian fluid. Since the recoverable shear for a viscoelastic fluid is zero at the centerline, while a maximum at the wall, there may be an off-axis radial position where swell is its greatest when convoluted with streamline rearrangement. This effect could affect the strength of a 3D printed part, due to molecular orientation and its gradient, and should be considered. In fact, the nozzle exit could be profiled in a way to promote or inhibit die swell.

Note, Eq. (6) is only valid for a viscometric flow where entrance effects are negligible [42]. A capillary length on diameter ratio of order 20 is necessary for this. A condition like this will never exist in ME, so, the entry region within the nozzle must be included promoting sophisticated modeling and rheological knowledge of the material. What rheological properties should a material have to limit or promote die swell under these conditions? Can die swell be incorporated into the printer's control algorithm? Die swell is expected to be quite large since the apparent shear rate ($8V_d/d$, see Table I) in the nozzle's capillary is order 400 s^{-1}. Yet, the nozzle exit is very close to the substrate which may inhibit swelling perhaps increasing stress and orientation in the printed part as it spreads the melt onto the underlaying material. Will this effect occur and how will it affect the part strength? Finally, many polymer melts are filled and the effect of fillers on die swell is complicated, [43] what will be the die swell for these type of materials in ME given the restrictions of the flow geometry?

VI. HEALING

When a track (or road) of polymer is deposited onto a previously deposited one two phenomena happen; they wet each other and the interface disappears. Of course, the disappearance is through molecular diffusion of the polymer molecules which is described by a repation mechanism [44, 45]. This healing process promotes a stronger 3D printed part so rheological properties such as the tensile stress or tear strength increase, for example, that are integral to success of this technology. How healing occurs in ME is not obvious so a description of healing under more controlled conditions is given below and then conjecture to the real processing conditions and how other rheological properties may affect it are considered.

The time t dependent degree of healing $D(t)$ of a (mechanical) property $P(t)$ is given by [10]

$$D(t) = \frac{P(t)}{P_\infty} = \int_{-\infty}^{t} R_{\rm h}(t-\tau) \times \frac{d\phi(\tau)}{d\tau}\, d\tau \qquad (7)$$

where P_∞ is the property's value after an infinite healing time. The intrinsic healing function $R_{\rm h}(t)$ is ultimately related to macromolecular diffusion, and will be discussed below, while $\phi(t)$ is the wetted areal fraction of the two-dimensional system after correcting for impingement of the growing wetted areas. The wetted areas can be thought to be *patchy* circular regions where the two interfaces make intimate contact that grow in the radial direction with time.

Wetting must occur before diffusion and Wool and O'Connor discuss the different wetting types where only instantaneous is considered here. In this case one has $d\phi(t)/dt = \delta(t)$ and the above equation simplifies to

$$D(t) = D_0 + R_{\rm h}(t)$$

where D_0 was added and represents the instantaneous healing that will occur upon intimate contact (*i.e.* this may be due to *van der Waals* forces between the intimately wetted surfaces). Diffusion arguments under the reptation assumption can be made to find $R_{\rm h}(t) \propto t^{1/4}$ for a property such as the fracture strength or equivalently the critical fracture toughness $K_{\rm Ic}$.[2] Some care in using the $t^{1/4}$ power law should be made since Wool and co-workers show the healing power law does depend on the molecular weight used [46].

The above analysis is valid for isothermal conditions. Material extrusion is certainly not isothermal since Seppala and Migler [47] show the Acrylonitrile Butadiene Styene (ABS) copolymer blend's interface is below the glass transition temperature within 2 sec. of extrusion from the nozzle. Of course, once the glass transition temperature is reached diffusion is arrested. Before that, on initial contact, the interfacial temperature of the deposited *hot* material on the previously placed *cold* track immediately changes to exactly the average of the two,

[2] If the critical strain energy release G_{Ic} is measured one will have $t^{1/2}$ for time dependent healing since $G_{Ic} \propto K_{Ic}^2$

so, there is an initial rapid cooling of the melt, at least at the interface. The two tracks then cool over a fairly short time period where the viscosity and reptation time rapidly increase.

The above analysis cannot be used under nonisothermal conditions and fortunately Yang and Pitchumani [48] have performed theory and experiment where the temperature is not constant, with the wetted areal fraction is constant, and find

$$D(t) = \left[\int_0^t \frac{1}{\tau_w(T(t))}\, dt\right]^{1/4} \tag{8}$$

where τ_w is called the weld time by Yang and Pitchumani. Their argument is the mechanical property may come to its infinite time value before the reptation time required for interfacial healing and this should be used. So, according to their analysis, the degree of healing should be measured isothermally at a given temperature to build a data base of $\tau_w(T)$ that can be substituted into the above equation for a given temperature profile.

In reality, during the welding process in ME, the time above the glass transition is very short, of order 1 sec., and it will be difficult to measure $\tau_w(T)$ and to ascertain whether this is the correct time scale to use when the temperature changes so rapidly. It is recommended to use the reptation time, which represents the time it takes a given polymer molecule to fully achieve a new set of constraints, in Eq (8). This, of course, deserves study and the rheologically derived reptation time should be measured and used in Eq (8) for comparison to macroscopically determined fracture properties of 3D printed test specimens. McIlroy and Olmsted [49] have done this and also considered how upstream shear affects the ultimate weld strength since shear can affect the reptation time. Further research from both theoretical and experimental approaches [50] are required.

ME suffers in widespread utility in engineering applications since the final product strength is inferior to those made by Selective Laser Sintering (SLS). The SLS process allows *in situ* annealing of powder to make stronger products suggesting that a post-processing annealing step of ME parts will make them stronger too (note the SLS process is very different to ME and a laser is used to melt the deposited polymer layer which also melts the layer below allowing a good weld to form). Although the user selects the *fill* level, that is the voidage, when ME is used this does not necessarily mean a 100% fill level has no voids because the extruded cylindrical tracks cannot relax nor expel air before they solidify [51].

Thomas and Rodriguez [52] studied how post-processing thermal annealing increased part strength. The principle is that further interfacial annealing will occur as well as an increase in the contact area. They used Wool and O'Connor's model [10] convoluted with a wetting model that was a stretched exponential. Contemporary wetting models reference Frenkel [53] and Eshleby

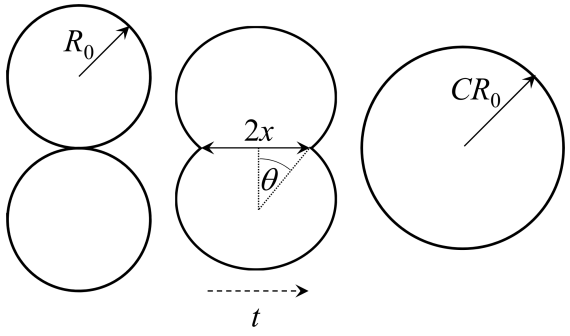

FIG. 8. Geometric variables used to describe the sintering of two fluid cylinders driven by surface tension. The cylinders have an initial radius of R_0 and after sintering the radius of the combined cylinders is $C \times R_0$.

[54] [3] that is the standard for all models even though it was derived for the sintering of two spheres. As it turns out the Frenkel-Eshleby model is the short time asymptote for a more refined consideration (see [55]) and is written

$$\theta = \left[\frac{t}{t_c}\right]^{1/2} \qquad \text{(spheres)}$$

with reference to Fig. 8 for the definition of geometric variables and C is $\sqrt[3]{2}$ for the sintering of spheres and $\sqrt{2}$ for cylinders due to the conservation of mass. The characteristic time t_c is $\eta R_0/\mathcal{S}$ with η being the (Newtonian) viscosity and $\mathcal{S}$ the surface tension.

Much of the research in the polymer sintering area has centered on spheres, however, 3D printing requires an analysis for the sintering of cylinders. This was done by Hopper [56] (see also Pokluda *et al.* [55]) assuming Newtonian flow behavior who found different asymptotic behavior to that of spheres

$$\frac{t}{t_c} = \pi\,\hat{x}\,\left[\frac{1}{\Lambda} - \frac{1}{\Lambda^2} + \frac{2}{\Lambda^3}\right] \qquad t \to 0$$

and

$$\frac{t}{t_c} = -0.3218 - \ln(1-\hat{x}) \qquad t \to \infty$$

where $\hat{x} = x/\sqrt{2}R_0$ and $\Lambda = \ln(16/[1-\hat{x}^2])$. Hopper also determined an empirical relation

$$\hat{x} = 0.779\left[\frac{t}{t_c}\right]^{0.857} \qquad \text{(cylinders)}$$

[3] The contribution of Eshleby comes in the discussion of the paper by Shaler where he corrects Frenkel's analysis stating that flow within two sintering particles is elongation-like and not shear-like.

for $0.003 < \hat{x} < 0.15$ which has a very different power law to the sintering of spheres.

Now, assuming the rate of interfacial contact area increase during post-printing annealing is slow, macromolecular diffusion will not be the limiting step and one expects from Eq. 7

$$D(t) = \phi_0 + \phi(t)$$

where ϕ_0 is the initial contact area prior to annealing. Thus, the part becomes stronger during annealing since the contact area, which is proportional to x, increases. It is clear there is a difference in the healing temporal behavior between spherical and cylindrical geometries and a full analysis for the most appropriate geometry in ME should be performed. The challenge is to understand healing from a rheological point of view since annealing should be done as quickly as possible suggesting elongational flow may be important since an increase in x provides a stretching flow.

The type of elongational flow between two sintering spheres is uniaxial and similar to two jets impinging on each other. However, the elongational flow between two cylinders is more similar to planar elongational flow, although not exactly. A consideration is that planar elongational flow is neutrally aligning, just like shear flow, and not a *strong flow* [57] and has implications as to whether viscoelasticity comes fully into play. Bellehumer *et al.* [58] show viscoelasticity retards sintering of spheres quite significantly and this could have an effect in the annealing rate. Yet, Hart *et al.* [59] have performed annealing of 3D printed parts and found their strength could be significantly increased, so, post-printing annealing can be a viable technology to improve the mechanical properties.

As mentioned above, processing aids could be introduced to a material allowing faster extrusion rates, how will they affect healing? Will they reduce or increase the initial wetting? Will they affect diffusion at the interface? Finally, upstream conditions promote orientation *via* flow in the conical nozzle, this this affect polymer diffusion under ME conditions? These are questions that should be answered to ensure that their introduction improves the overall process and not just the extrusion aspect.

VII. OTHER CONSIDERATIONS

Filament break-up. The 3D printing process consists of extruding a molten polymer filament onto a track for a given horizontal distance then the nozzle is lifted, the fiber is retracted to slightly pull on the extruded filament and the nozzle moved to another position and the deposition process is repeated. Occasionally the filament will not cleanly *break* from the deposited track and a *spider web* can be seen on the object as the thinning polymer filament traces the nozzle movement and falls onto the already deposited tracks. This is clearly undesirable and should be avoided if at all possible. We draw from two disparate research areas to understand this phenomenon and how to avoid it; fiber spinning and fluid dispensing.

Polymer processing of melts to make fibers requires that the material be *spinnable*, meaning that the extruded melt does not break-up and a smooth diameter reduction from the spinneret is possible to produce the given gauge fiber. Han [60] considered the spinnability of polymer solutions and melts *via* a theoretical analysis using a viscoelastic equation of state together with a force balance. Before doing this he surveyed the literature in great detail and concluded that neither the viscosity nor the surface tension ($\mathcal{S}$) influenced the break-up of fibers as they were spun. His theoretical analysis then centered on how elasticity lead to stability during spinning with greater elasticity producing the most spinnable melt. Obviously one does not desire a very elastic polymer melt in ME since the filament will not break from the deposited track, yet, how elastic can it be? This leads to the other research area discussed by Clasen *et al.* [61]

Clasen *et al.* [61] assessed the forces that led to dispensing a drop or having jetting occur. Jetting is equivalent to producing a stable fiber that does not break. In their study they want the extrudate to break and a drop formed so it can be dispensed in ink jet printing, for example, while Han [60] does not desire break-up. A series of experiments were conducted by Clasen *et al.* to determine what dimensionless forces are the most important to produce a drop rather than a jet and they determined the *map of misery* consisting of a three dimensional graph of the relevant dimensionless numbers dictating break-up.

Three dimensionless numbers of importance are We, the Weber number, Ca, the capillary number and Wi, the Weissenberg number defined as

$$We \equiv \frac{\rho V_{\rm d}^2 d}{\mathcal{S}} \approx 0.01,\; Ca \equiv \frac{\eta V_{\rm d}}{\mathcal{S}} \approx 5,000,\; Wi \equiv \frac{\lambda V_{\rm d}}{d} \approx 1$$

with the geometric and processing variables given in Fig. 3 and Table I while ρ is the density and λ is the viscoelastic fluid's relaxation time (the diameter is used as the relevant length scale here while Clasen *et al.* used the radius, also die swell and its effect on filament diameter has been ignored). The order of magnitude for each dimensionless number is given above and it is clear that We, the ratio of inertial to surface tension forces, is very small while Ca, the ratio of viscous to surface tension forces, is quite large. However, Wi, the ratio of an elastic to processing time scale, is of order one suggesting this could be an important number dictating filament break-up in ME since Ca will always be very large for polymer melts.

However, further insight can be made by considering two other dimensionless numbers. The Ohnesorge number ($Oh = Ca/\sqrt{We} > 10^4$) which balances viscous and inertial forces and the Elasto-Capillary number ($Ec \equiv Wi/Ca < 10^{-2}$) that is a dimensionless relation between viscous and elastic effects. Due to their magnitude, Clasen *et al.* suggest polymer melts are weakly

elastic liquids and viscosity will dominate the break-up response. This is opposite to what Han indicates where elasticity is the dominate parameter dictating break-up.

Thus, the two research fields have different conclusions as to what dictates filament break-up necessitating further thought and research. Also, one should realize ME is nonisothermal, as will be fiber spinning of polymer melts, which certainly affects break-up and deserves further study under controlled conditions. In addition, research needs to be performed through the lens of examining the elongational flow properties, which is the relevant elasticity inducing deformation in ME, to determine its influence on break-up.

Orientation. In contemporary polymer processing, a molten fiber is extruded then a series of stretching operations performed to yield the correct diameter while simultaneously imparting strength through orientation. The ratio of the pulling (take-up) velocity to the average velocity in the capillary is called the draw ratio DR. The DR is an important parameter in any extrusion operation and will be so in ME.

McIlroy and Olmsted [62] have found the curvature ρ_t (see Fig. 3) when the filament translates from the nozzle exit to laying on the already deposited track can affect the polymer orientation. Presently, it is unknown what the curvature is and how it is affected by the material rheological properties especially since it can be affected by die swell. Also, pulling the deposited track can create orientation and is measured by the draw ratio

$$\mathrm{DR} = \frac{V_t}{V_d} \approx 2$$

where the approximate value comes by using typical values in Table I. It is unknown how this affects the molecular orientation in the final 3D printed object. Indeed it is unknown how large the molecular orientation is for any 3D printed part and this should be measured by neutron scattering or similar and related to the processing and rheological properties.

As implied in the above discussion, orientation in the 3D printed object is hypothesized to be important in the final object's strength. Certainly, the weld strength discussed above is also important, yet, if this can be enhanced then orientation will affect the part strength. Can orientation developed within the nozzle be retained and translated to a much stronger printed part by optimization and understanding of the rheological and processing parameters? However, annealing was discussed above and suggested to be a way to increase strength, yet, if a printed object is annealed then orientation will be lost. Thus, there could be an interplay between retaining processing based orientation and annealing to increase the contact area between tracks requiring significant rheological knowledge of the material and its interaction with processing.

Finally, the set-up of a ME instrument requires the nozzle to be approximately 100 μm from the bed before printing is started. This is the *zero* set point. This set point is usually determined by placing a piece of paper on the bed and moving the nozzle down until the paper can no longer be easily moved. This leaves a gap Δ between the nozzle and extruded tracks, see Fig. 3. How does this seemingly arbitrary distance affect orientation in the 3D printed part as well as *healing*? This certainly deserves some attention as more comprehensive research is performed on ME.

Reinforcement. There are printers that can use continuous or short fibers to improve the strength of printed parts. Different ways are used to incorporate continuous fiber, it can be supplied to the nozzle assembly and co-printed with the polymer or it can be placed onto the substrate with another print head and the matrix printed on top of it with the process repeated as the object is fabricated [63]. Filled materials certainly present rheological challenges while the separate continuous fiber – matrix technique presents wetting issues.

It was mentioned above that fillers can affect die swell and this is, of course, a rheological phenomenon. However, the addition of solid particles to a viscoelastic fluid produces unusual effects compared to a Newtonian carrier fluid [64]. The standard scaling relations for the viscosity fail and must be modified while viscoelastic effects are at times counterintuitive. Now, this unusual behavior coupled with processing in a confined geometry (*i.e.* the small diameter of the capillary in the nozzle) will assuredly generate a host of interesting observations. For example, will short fibers be completely oriented in the flow direction? How uniformly dispersed will the fillers be? Will the state of dispersion affect the part strength? Will particles affect the wetting and diffusion phenomena discussed above? These and many other questions are relevant to the effect of reinforcement on the process and products made by ME.

VIII. CONCLUSION

A review of the rheological behavior present in ME has been presented to highlight its importance. There are clearly opportunities for improvement in the process necessitating careful rheological measurement, interpretation, simulation and optimization to achieve stronger 3D printed objects in a timely manner. Although the polymers currently used in Additive Manufacture have been thoroughly reviewed [65] there is no possibility to comment on their rheological properties and how they interact with the process in any detailed fashion at this point in time. There is clearly a need for a concerted rheology-centric investigation of ME to allow process and instrument development to overcome the shortcomings of ME; long build times and reduced strength of 3D printed parts.

SUPPLEMENTARY MATERIAL

See supplementary material for a more detailed discussion of the Graetz solution to the heat transfer of a fluid flowing in a heated/cooled pipe.

ACKNOWLEDGMENTS

I am grateful for a grant from the Army Research Laboratory under award W911NF-17-2-0186 to study material extrusion and the help of Aleph Objects, Inc. - Makers of LulzBot 3D Printers.

[1] Y. Huang, M.C. Leu, J. Mazumder, and A. Donmez, "Additive manufacturing: Current state, future potential, gaps and needs, and recommendations," J. Manu. Sci. Eng. **137**, 014001–1–10 (2015).

[2] I.S. Hyatt and J.W. Hyatt, "Improvement in processes and apparatus for manufacturing pyroxyline," U.S. Patent No. 133,229 (1872).

[3] J.W. Hyatt, "Address of acceptance," Ind. Eng. Chem. **6**, 158–161 (1914).

[4] B. Wendel, D. Rietzel, F. Kuhnlein, R. Feulner, G. Hulder, and E. Schmachtenberg, "Additive processing of polymers," Macrom. Mat. Eng. **293**, 799–809 (2008).

[5] A. Lazarus, J.T. Miller, and P.M. Reis, "Continuation of equilibria and stability of slender elastic rods using an asymptotic numerical method," J. Mech. Phys. Solids **61**, 1712–1736 (2013).

[6] J. Go, S.N. Schiffres, A.G. Stevens, and A.J. Hart, "Rate limits of additive manufacturing by fused filament fabrication and guidelines for high-throughput system design," Add. Manu. **16**, 1–11 (2017).

[7] D.G. Baird and D.I. Collias, *Polymer processing: Principles and design* (Wiley, Hoboken, 2014).

[8] Z. Tadmor and C.G. Gogos, *Principles of polymer processing, 2nd edition* (John Wiley and Sons, Hoboken, N.J., 2006).

[9] J. F. Agassant, D. R. Arda, C. Combeaud, A. Merten, H. Munstedt, M. R. Mackley, L. Robert, and B. Vergnes, "Polymer processing extrusion instabilities and methods for their elimination or minimisation," Intern. Poly. Proc. **21**, 239–255 (2006).

[10] R. P. Wool and K. M. O'Connor, "A theory of crack healing in polymers," J. App. Phys. **52**, 5953–5963 (1981).

[11] F. Yang and R. Pitchumani, "Healing of thermoplastic polymers at an interface under nonisothermal conditions," Macromolecules **35**, 3213–3224 (2002).

[12] A. M. Kraynik and W. R. Schowalter, "Slip at the wall and extrudate roughness with aqueous-solutions of polyvinyl-alcohol and sodium-borate," J. Rheol. **25**, 95–114 (1981).

[13] B. T. Atwood and W. R. Schowalter, "Measurements of slip at the wall during flow of high-density polyethylene through a rectangular conduit," Rheol. Acta **28**, 134–146 (1989).

[14] F. J. Lim and W. R. Schowalter, "Wall slip of narrow molecular-weight distribution polybutadienes," J. Rheol. **33**, 1359–1382 (1989).

[15] J. Go and A.J. Hart, "Fast desktop-sclae extrustion additive manufacturing," Add. Manu. **18**, 276–284 (2017).

[16] D.D.. Phan, Z.R. Swain, and M.E. Mackay, "Rheological and heat transfer effects in fused filament fabrication," J. Rheol. **62**, 1097–1107 (2018).

[17] W.H. McAdams, *Heat Transmission*, 3rd ed. (McGraw-Hill, New York, 1954).

[18] R. G. Griskey and I. A. Wiehe, "Heat transfer to molten flowing polymers," AIChE J. **12**, 308–312 (1966).

[19] I. Saltuk, N. Siskovic, and R. G. Griskey, "Energy transport to molten flowing polymer systems - .2. analysis of data and development of temperature profiles with axial length," Poly. Eng. Sci. **12**, 402–408 (1972).

[20] T. B. Drew, "Mathematical attacks on forced convection problems a review," Trans. Amer. Inst. Chem. Eng. **26**, 26–80 (1931).

[21] A. B. Metzner, R. D. Vaughn, and G. L. Houghton, "Heat transfer to non-newtonian fluids," AIChE J. **3**, 92–100 (1957).

[22] M. Hu, P. Keblinski, and P. K. Schelling, "Kapitza conductance of silicon-amorphous polyethylene interfaces by molecular dynamics simulations," Phys. Rev. B **79**, 104305–1–7 (2009).

[23] Xingfei Wei, Teng Zhang, and Tengfei Luo, "Thermal energy transport across hard-soft interfaces," ACS Energy Letters **2**, 2283–2292 (2017).

[24] S. Middleman, *Fundamentals of polymer processing* (McGraw-Hill Book Company, New York, 1977).

[25] Eric L. Gilmer, Darren Miller, Camden A. Chatham, Callie Zawaski, Jacob J. Fallon, Allison Pekkanen, Timothy E. Long, Christopher B. Williams, and Michael J. Bortner, "Model analysis of feedstock behavior in fused filament fabrication: Enabling rapid materials screening," Polymer **in press** (2017).

[26] F. N. Cogswell, "Converging flow of polymer melts in extrusion dies," Poly. Eng. Sci. **12**, 64–73 (1972).

[27] F. N. Cogswell, "Measuring extensional rheology of polymer melts," Trans. Soc. Rheol. **16**, 383–403 (1972).

[28] E. B. Bagley and H. P. Schreiber, "Effect of die entry geometry on polymer melt fracture and extrudate distortion," Trans. Soc. Rheol. **5**, 341–353 (1961).

[29] H. K. Nason, "A high temperature, high pressure rheometer for plastics," J. App. Phys. **16**, 338–343 (1945).

[30] N. ElKissi, J. M. Piau, and F. Toussaint, "Sharkskin and cracking of polymer melt extrudates," Journal of Non-Newtonian Fluid Mechanics **68**, 271–290 (1997).

[31] R. L. Boles, H. L. Davis, and D. C. Bogue, "Entrance flows of polymeric materials - pressure drop and flow patterns," Poly. Eng. Sci. **10**, 24–31 (1970).

[32] T. H. Kwon, S. F. Shen, and K. K. Wang, "Pressure-drop of polymeric melts in conical converging flow - experiments and predictions," Poly. Eng. Sci. **26**, 214–224 (1986).

[33] S. Middleman and J. Gavis, "Expansion and contraction of capillary jets of newtonian liquids," Phys. Fluids **4**, 355–359 (1961).

[34] J. Gavis and M. Modan, "Expansion and contraction of jets of newtonian liquids in air - effect of tube length," Phys. Fluids **10**, 487–497 (1967).

[35] J. Vlachopoulos, M. Horie, and S. Lidorikis, "Evaluation of expressions predicting die swell," Transactions of the Society of Rheology **16**, 669–685 (1972).

[36] C. Barus, "Isothermals, isopiestics and isometrics relative to viscosity," Am. J. Sci. (3) **45**, 87–96 (1893).

[37] A. C. Merrington, "Flow of visco-elastic materials in capillaries," Nature **152**, 663–663 (1943).

[38] A.B. Metzner, "Historical comments on stress relaxation following steady flows through a duct or orifice," Trans. Soc. Rheo. **13**, 467–470 (1969).

[39] R.I. Tanner, "A theory of die-swell," J. Poly. Sci. Part A-2 **8**, 2067–2078 (1970).

[40] S. Richardson, "The die swell phenomenon," Rheo. Acta **9**, 193–199 (1970).

[41] R. I. Tanner, "A theory of die-swell revisited," Journal of Non-Newtonian Fluid Mechanics **129**, 85–87 (2005).

[42] E.B. Bagley, S.H. Storey, and D.C. West, "Post extrusion swelling of polyethylene," J. App. Poly. Sci. **7**, 1661–1672 (1963).

[43] T. Nishimura and T. Kataoka, "Die swell of filled polymer melts," Rheol. Acta **23**, 401–407 (1984).

[44] S. F. Edwards, "Statistical mechanics of polymerized material," Proc. Phys. Soc. London **92**, 9–19 (1967).

[45] P. G. de Gennes, "Reptation of a polymer chain in presence of fixed obstacles," J. Chem. Phys. **55**, 572–579 (1971).

[46] R. P. Wool, B. L. Yuan, and O. J. McGarel, "Welding of polymer interfaces," Poly. Eng. Sci. **29**, 1340–1367 (1989).

[47] J. Seppala and K. Migler, "Infrared thermography of welding zones produced by polymerextrusion additive manufacturing," Add. Manu. **12**, 71–76 (2016).

[48] F. Yang and R. Pitchumani, "Healing of thermoplastic polymers at an interface under nonisothermal conditions," Macromolecules **35**, 3213–3224 (2002).

[49] C. McIlroy and P.D. Olmsted, "Disentanglement effects on welding behaviour of polymer melts during the fused-filament-fabrication method for additive manufacturing," Polymer **123**, 376–391 (2017).

[50] J. E. Seppala, S. H. Han, K. E. Hillgartner, C. S. Davis, and K. B. Migler, "Weld formation during material extrusion additive manufacturing," Soft Matter **13**, 6761–6769 (2017).

[51] Q. Sun, G. M. Rizvi, C. T. Bellehumeur, and P. Gu, "Effect of processing conditions on the bonding quality of FDM polymer filaments," Rapid Proto. J. **14**, 72–80 (2008).

[52] J.P. Thomas and J.F. Rodriguez, "Modeling the fracture strength between fused-deposition extruded roads," 11th Int. Freeform Fab. Symp. , 16–23 (2000).

[53] J. Frenkel, "Viscous flow of crystalline bodies under the action of surface tension," J. Phys. **9**, 385–391 (1945).

[54] A.J. Shaler, "Seminar on the kinetics of sintering," Metals Trans. **185**, 796–813 (1949).

[55] O. Pokluda, C. T. Bellehumeur, and J. Vlachopoulos, "Modification of frenkel's model for sintering," AIChE J. **43**, 3253–3256 (1997).

[56] R.W. Hopper, "Coalescence of two equal cylinders: exact results for creeping viscous plane flow driven by capillarity," J. Am. Ceram. Soc. (Comm) **67**, C–262–C–264 (1984).

[57] R.G. Larson, *Constitutive equations for polymer melts and solutions* (Butterworths, Boston, 1988) p. 364.

[58] Celine T. Bellehumeur, Marianne Kontopoulou, and John Vlachopoulos, "The role of viscoelasticity in polymer sintering," Rheol. Acta **37**, 270–278 (1998).

[59] Kevin Hart, Ryan M Dunn, Jennifer M Sietins, Clara M Hofmeister-Mock, Michael E Mackay, and Eric D Wetzel, "Increased fracture toughness of additively manufactured amorphous thermoplastics via thermal annealing," Polymer (submitted).

[60] C.D. Han, "A theoretical study on fiber spinnability," Rheo. Acta **9**, 355–365 (1970).

[61] C. Clasen, P. M. Phillips, L. Palangetic, and J. Vermant, "Dispensing of rheologically complex fluids: The map of misery," AIChE Journal **58**, 3242–3255 (2012).

[62] C. McIlroy and P. D. Olmsted, "Deformation of an amorphous polymer during the fused-filament-fabrication method for additive manufacturing," J. Rheo. **61**, 379–397 (2017).

[63] R. Matsuzaki, M. Ueda, M. Namiki, T. K. Jeong, H. Asahara, K. Horiguchi, T. Nakamura, A. Todoroki, and Y. Hirano, "Three-dimensional printing of continuous-fiber composites by in-nozzle impregnation," Sci. Reports **6** (2016), ARTN 23058.

[64] A. B. Metzner, "Rheology of suspensions in polymeric liquids," J. Rheol. **29**, 739–775 (1985).

[65] S. C. Ligon, R. Liska, J. Stampfl, M. Gurr, and R. Mulhaupt, "Polymers for 3d printing and customized additive manufacturing," Chem. Rev. **117**, 10212–10290 (2017).